

1 **Supplementary materials of**

2 **Carbon reduction requires attention to the contribution of natural gas**
3 **use: combustion and leakage**

4

5

6

7

8 NUMBER OF PAGES:13

9 NUMBER OF FIGURES:9

10 NUMBER OF TEXTS:4

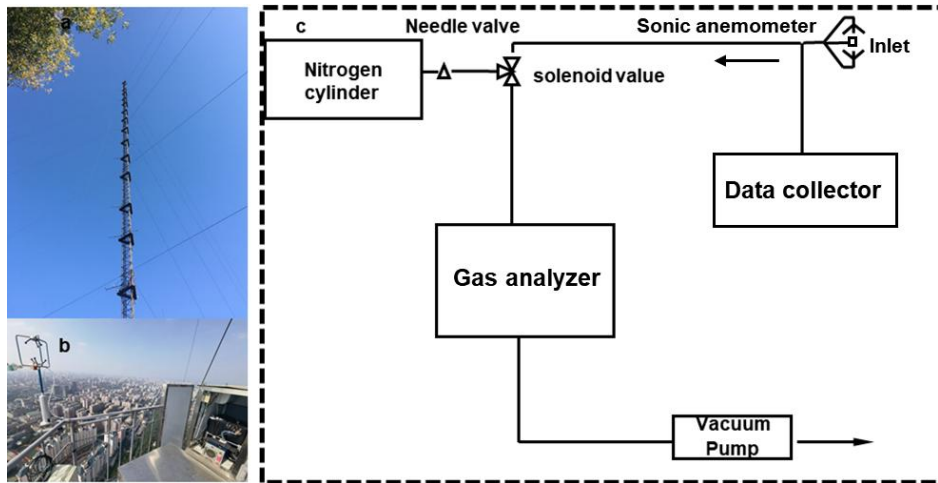
11

12 This supplementary information contains about details about Beijing Meteorological Tower, eddy
13 observation system and navigation observation station, daily summer variation of CO₂ flux from
14 2009 to 2017, the total consumption, electricity inflow and the proportion of natural gas in total
15 energy consumption from 2013-2022, the spatial distribution of CO₂ and CH₄ flux with wind
16 speed and direction, grid distribution of natural gas consumption in Beijing, calculation methods
17 of flux source area and natural gas leakage rate, uncertainty analysis of flux calculation, estimation
18 of non-natural gas sources

19

20

21



22
 23 Figure. S1 Beijing Meteorological Tower(a), Eddy Observation System(b) and Schematic
 24 Diagram(c)

25
 26
 27 **Text S1 Calculation methods of flux source area**

28 Eddy covariance method belongs to single point observation, so the observation results at a
 29 certain height can only reflect the information of a specific area around the site. The area where
 30 the upwind direction of the observation site contributes to the measured flux is called the flux
 31 contribution source area. For a homogeneous underlying surface, the flux from all directions and
 32 distances around the observation point is the same, so the contribution of flux to the source area is
 33 not a major issue to consider. However, for the heterogeneous underlying surface studied in this
 34 article, as the wind direction and speed change over time, the measured flux comes from different
 35 directions and distances around the observation points, including the flux contributions of
 36 different underlying surface patches. Therefore, the analysis of spatial representativeness in flux
 37 observations is particularly important. The flux footprint model can be used to quantitatively
 38 analyze the range of flux contribution source regions. The flux footprint function estimates the
 39 position and relative importance of the flux source that affects a given height of flux observation
 40 based on observation height, atmospheric stability, and surface roughness, expressed as a set of
 41 distances between observation points and flux sources in different directions, the specific

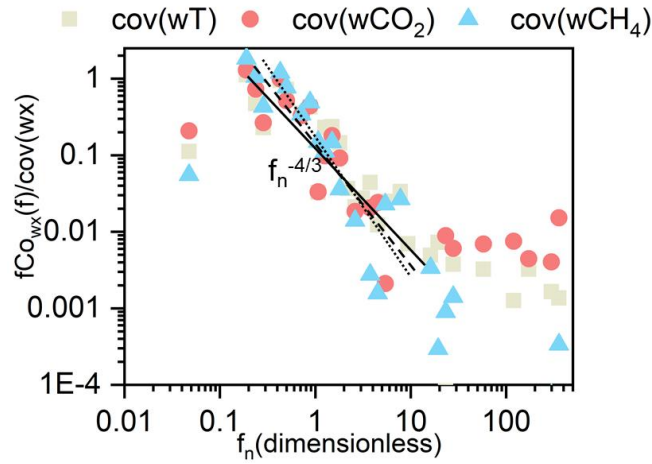
42 calculation formula is as follows:

$$x_{peak} = X_{peak}^* z_m \left(\frac{\sigma_w}{u_*} \right)^{-0.8}$$

$$x_{nn\%} = X_{nn\%}^* z_m \left(\frac{\sigma_w}{u_*} \right)^{-0.8}$$

43 Among them, x_{peak} refers to contributing distance to maximum flux, $x_{nn\%}$ refers to contributing
 44 distance to nn% flux, X_{peak}^* and $X_{nn\%}^*$ refer to the dimensionless distance related to surface
 45 roughness, z_m refers to observation altitude, σ_w refers to the standard deviation of vertical wind
 46 speed, u_* refers to friction wind speed.

47



48

49 Figure. S2 Normalized cospectra of T(sonic temperature), CO₂ and CH₄ with respect to w(vertical
 50 wind component). The normalized frequency f_n is defined as $f_n = f(z-d)/U$, where z, d and U denote
 51 measurement height(m), zero plane displacement(m) and wind speed(m/s), respectively. Each
 52 cospectrum is an average of half-hourly cospectra between 12:00-16:00. Regression of spectra for
 53 f_n between 0.1-10Hz marked by solid line for $Co(wT)$ and dashed line for both $Co(wCO_2)$ and
 54 $Co(wCH_4)$

55

56

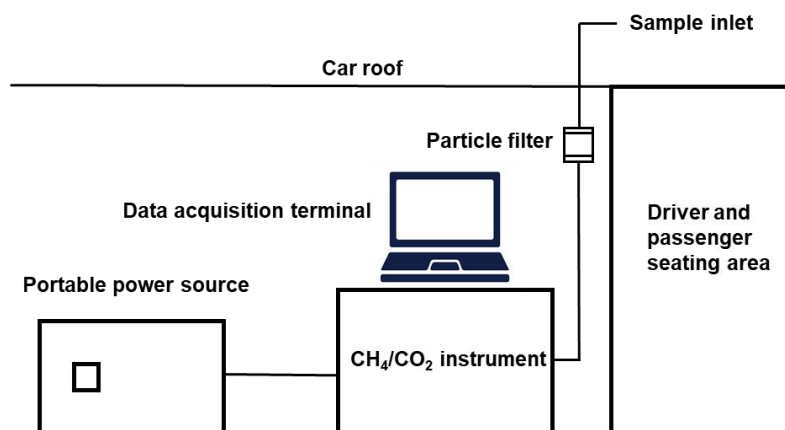


Figure. S3 Schematic diagram of navigation observation station

Text S2 The uncertainty analysis of flux calculation

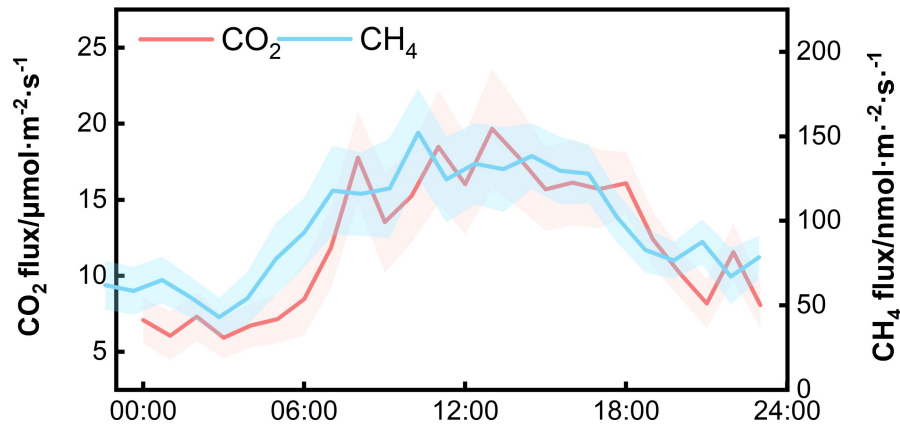
Just like other complex observations, flux observations based on eddy covariance method are subject to both systematic and random errors. However, different many other observations, it cannot be directly calibrated on-site for the measured flux. In addition to systematic errors caused by instrument calibration and data processing, sampling errors are one of the largest sources of uncertainty in vortex related flux observations. Sampling errors cannot be eliminated through experimental design due to the limited number of independent samples that contribute significantly to the flux within any fixed sampling period, and there are various auto-correlations and cross-correlations in the two covariates. A longer sampling period will increase the number of independent samples, thereby reducing sampling errors, but it often leads to other problems such as lack of atmospheric stability.

To answer questions such as whether any two flux observations varies significantly from each other, whether a specific flux observation is different from zero notably, and whether the flux observation is in alignment with the model results, it is necessary to quantify the contribution of sampling errors. We adopted the scheme proposed by Finkelstein and Sims (2001)¹ to calculate the sampling error, and the specific calculation formula is as follows:

$$\sigma_F = \sqrt{\frac{1}{n} \left[\sum_{p=-m}^m \gamma_{w,w}(p) \gamma_{c,c}(p) + \sum_{p=-m}^m \gamma_{w,c}(p) \gamma_{c,w}(p) \right]}$$

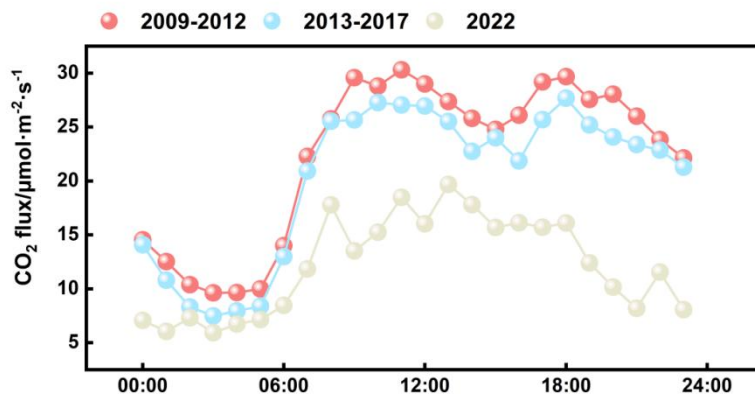
76 Where n is the number of samples within the average period of flux, m needs to be greater than
 77 the turbulent integration time scale, p is the lag time, and $\gamma_{w,w}(p)$ and $\gamma_{c,c}(p)$ refer to the
 78 auto-covariance of w and c , respectively.

79 Figure.S4 shows the daily variation and random error of CO_2 and CH_4 flux during the
 80 observation period. The range of random error for CO_2 flux is $1.43\text{-}3.72 \mu\text{mol}\cdot\text{m}^{-2}\cdot\text{s}^{-1}$, with a mean
 81 of $2.33 \mu\text{mol}\cdot\text{m}^{-2}\cdot\text{s}^{-1}$. The range of random error for CH_4 flux is $10.92\text{-}29.54 \text{nmol}\cdot\text{m}^{-2}\cdot\text{s}^{-1}$, with a
 82 mean of $18.43 \text{nmol}\cdot\text{m}^{-2}\cdot\text{s}^{-1}$. Both flux and random error peak between 10:00 and 15:00, when the
 83 absolute random error is large while the relative random error is small.



84
 85

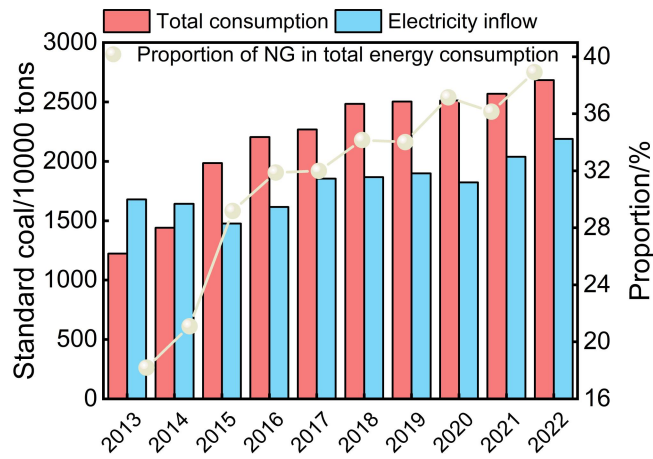
Figure.S4 The daily variation of CO_2 and CH_4 flux and their error bands



86

87

Figure.S5 Daily summer variation of CO₂ flux from 2009 to 2017 compared to this study



88

89

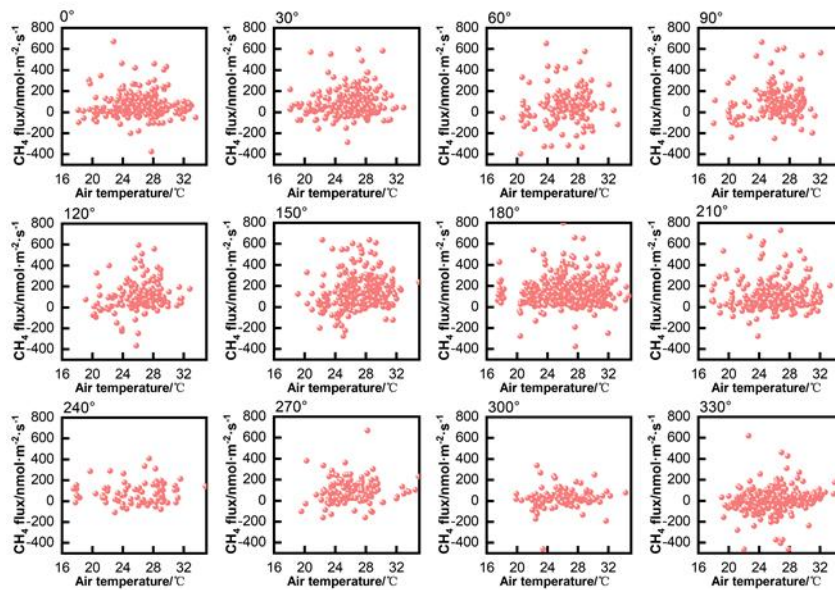
Figure. S6 The total consumption, electricity inflow and the proportion of natural gas in total

90

energy consumption from 2013-2022

91

92



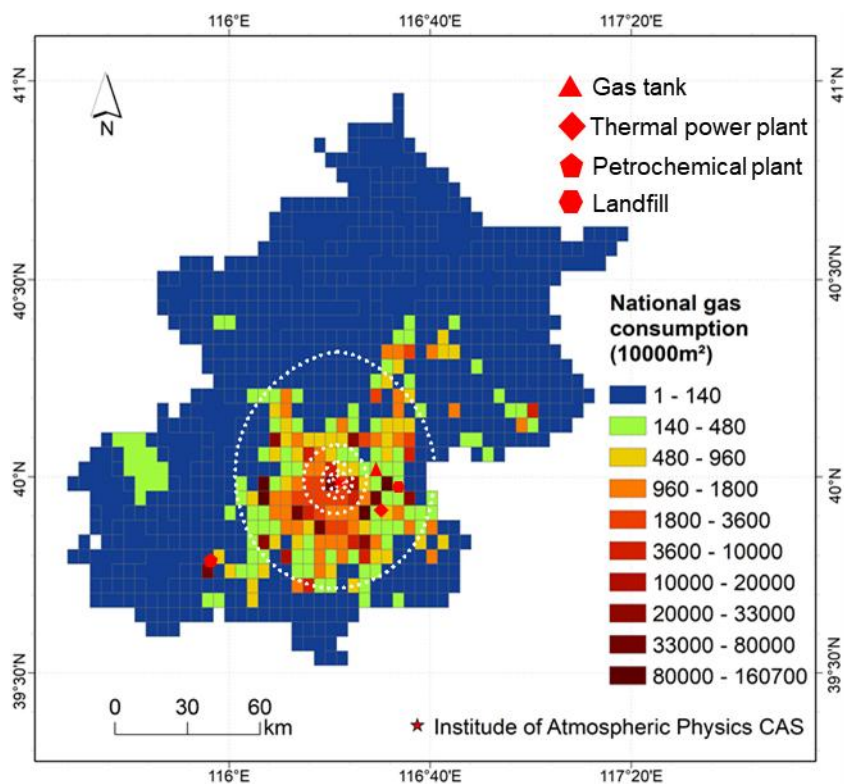
93

94

Figure. S7 Scatter plot of temperature and CH₄ flux along 12 directions

95

96



97

98 Figure.S8 Grid distribution of natural gas consumption in Beijing (the total residential
 99 consumption is gridded according to population density, the final grid result is the superposition of
 100 the enterprise and residential consumption, the white dotted line refers to the flux source area)

101

102 **Text S3 Calculation methods of natural gas leakage rate (LR)**

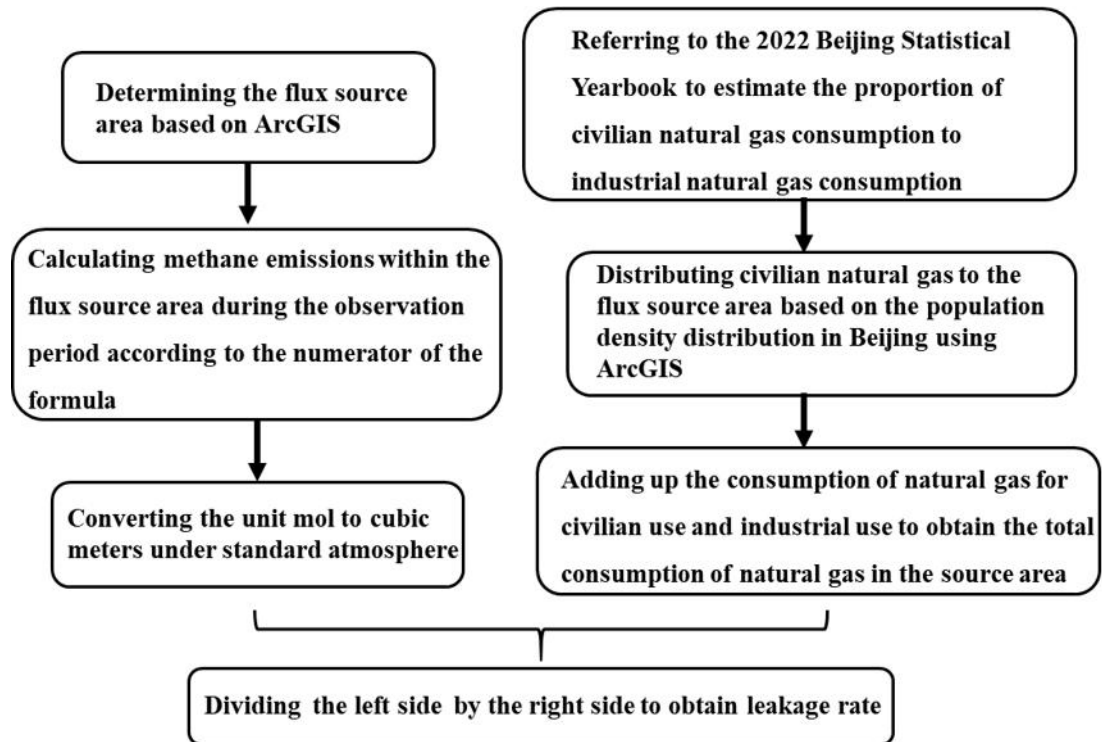
103

104
$$LR = \frac{Flux \times A \times F \times T}{NG_{sum}}$$

105 Among them, *LR* refers to methane leakage rate, *Flux* refers to CH₄ flux, *A* refers to area of flux
 106 source, *F* refers to factor converting amount of substance(mol) to volume(m³), *T* refers to
 107 Observation duration, *NG_{sum}* refers to sum of natural gas consumption during observation period
 108 within the flux source area. The following diagram shows the specific calculation steps.

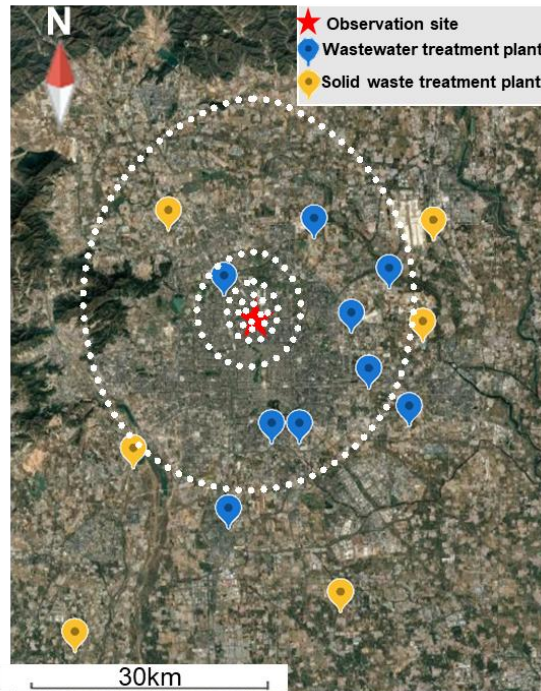
109 Considering that the natural gas consumption data of industry during the observation period was
 110 directly obtained by the Beijing Ecological Environment Center, the uncertainty of the total

111 natural gas consumption during the observation period mainly comes from civilian natural gas,
112 however, the annual consumption of civilian natural gas only accounts for about 10% of industrial
113 natural gas consumption in 2022. Therefore, we reckon that the uncertainty of natural gas leakage
114 rate based on this method is relatively small though civilian natural gas was evenly distributed
115 among observation durations without considering seasonal variability here.
116



117

118 **Text S4 Estimation of non-natural gas sources**



119

120 Figure.S9 Locations of large-scale sewage treatment plants and solid waste treatment plants in
 121 Beijing (the map was extracted from © Google earth: <https://earth.google.com/>)

122 The existing inventory shows that the waste treatment process mainly includes solid waste
 123 disposal, wastewater treatment (including anaerobic treatment of domestic and industrial
 124 wastewater, CH₄ emissions from sludge), which are important sources of methane in Beijing. The
 125 common methods of solid waste treatment include composting, incineration, and landfilling.
 126 Previous studies have shown that landfill treatment produces several orders of magnitude higher
 127 CH₄ than composting and incineration treatment.² Therefore, we mainly considered the methane
 128 emissions from landfilling treatment. Large-scale landfill sites in Beijing were selected here, it can
 129 be seen that most of them are not located within the flux source area (only one), so we assumed
 130 that methane emissions from garbage dumps within the source area could be approximately
 131 ignored (Figure.S10). However, methane emissions from wastewater treatment plants should be
 132 considered, as there distributed many sewage treatment plants within the source area (Figure.S10)
 133 with actual treatment capacities of over 40 million tons per year, which will make a certain
 134 contribution to methane emissions in the source area. In addition, urban sewage pipeline systems

135 also play an important role in methane emissions in cities, and CH₄ emissions from which in some
136 areas may be much higher than CH₄ emissions from sewage treatment plants.^{3,4}

137 Although based on current results, this contribution seemed relatively small compared to
138 natural gas. Firstly, if biogenic sources dominated methane emissions within the source area,
139 methane flux would show a high correlation with temperature. Hu et al.'s study indicated that a
140 10°C increase in temperature will lead to a 38%-50% increase in waste based methane
141 emissions,⁵ which contradicts our observations., for no correlation was observed between methane
142 flux and temperature in all directions (Figure.S7). Moreover, the observation experiments
143 conducted by Yin et al. at the Guiyang wastewater treatment plants showed that the methane
144 emission would peak at night considering that it was related to the wastewater treatment time and
145 hydraulic retention time,⁶ which was not reflected in our observation results.

146 The contribution of wastewater treatment plant emissions within the flux source area was
147 roughly estimated based on the results of the literature. According to Zhao et al.'s conclusion,⁷ the
148 total amount of methane emissions from urban sewage treatment plants correlated strongly with
149 the city's GDP, household consumption level and urban population density (correlation coefficient
150 is as high as 0.7-0.9), In megacities like Beijing, the per capita CH₄ emissions from urban sewage
151 treatment facilities can reach 2.9kg/year. According to the national census
152 results(<http://sedac.ciesin.columbia.edu//data/collection/gpw-v4/sets/browse>), the permanent
153 population of Beijing in 2022 is about 21.8 million, it is estimated that the population proportion
154 in the flux source area is 64.8% of the total population in Beijing using ArcGIS 10.2 on basis of
155 the world population grid data, with a corresponding population of approximately 14.1 million and
156 a flux source area of approximately 2400 square kilometers. The methane flux emitted from the
157 sewage treatment plants within the flux source area is approximately 12.35 nmol·m⁻²·s⁻¹, which
158 accounts for 13% of the methane flux during the observation period. As the CH₄ emissions during
159 wastewater treatment are significantly correlated with COD concentration. we also roughly
160 estimated its methane emissions based on emission factors. According to the estimates of Zhao et
161 al. for 229 cities in China,⁷ the CH₄ emission coefficient of urban sewage treatment plants is about

162 0.017-0.24gCH₄/gCOD, while the average per capita COD production in Chinese cities is
163 approximately 24kg/year.⁸ the emission flux of sewage treatment plants within the flux source area
164 is about 1.73-20.73nmol·m⁻²·s⁻¹ combining the flux source area and the population above, the flux
165 results calculated based on the correlation between CH₄ emission and population density are
166 within this range.

167 The methane emissions from urban sewer systems was estimated with the above emission
168 factor method. The CH₄ emission coefficient of urban sewage pipelines is about 0.0532
169 gCH₄/gCOD.⁸ Based on the area of the flux source area and the population in the source area, the
170 sewage pipeline flux is around 5 nmol·m⁻²·s⁻¹. Therefore, the total methane flux from wastewater
171 within the flux source area comes to 6.73-25.73 nmol·m⁻²·s⁻¹, and whose contribution to the
172 methane flux is the highest at 27%, making the lower limit of natural gas leakage in Beijing
173 estimate to be 0.82%, 1.12% can be used as the upper limit of natural gas leakage ratio if all
174 methane emissions are attributed to natural gas. Unfortunately, due to a lack of data, we are
175 currently unable to quantify the uncertainty of the calculation results. However, it can be
176 confirmed that natural gas is the main source of methane emissions within the flux source area.

177

178 **Text S5 Formula of natural gas leakage rate**

179

$$180 \ln \max excess CH_4 = -0.988 + 0.817 \times \ln \text{emission rate}$$

181

182 Where the maxexcess CH₄ is the maximum CH₄ enhancement concentration (ppm), the unit for
183 emission rate is g/min.

184

185

186

187

REFERENCES

188 (1) Finkelstein, P.L.; Sims, P.F. Sampling error in eddy correlation flux measurements. J Geophys

189 Res. 2001, 106 (D4), 3503-3509 DOI: 10.1029/2000JD900731.

190 (2) Cai B.F. Study on Methane Emission Characteristics of Landfills in China in 2012.
191 Environmental Engineering. 2016, 34 (2), 4. DOI:10.13205/j.hjgc.201602001.

192 (3) Kyung, D.; Kim, D.; Yi, S.; Choi, W.; Lee, W. Estimation of greenhouse gas emissions from
193 sewer pipeline system. Int. J. Life. Cycle. Assess. 2017, 22 (12), 1901-1911 DOI:
194 10.1007/s11367-017-1288-9

195 (4) Mannina, G.; Butler, D.; Benedetti, L. Greenhouse gas emissions from integrated urban
196 drainage systems: Where do we stand?. J Hydrol. 2018, 559, 307-314 DOI:
197 10.1016/j.jhydrol.2018.02.058

198 (5) Hu, C.; Zhang, J.; Qi, B.; Du, R.; Xu, X.; Xiong, H.; Liu, H.; Ai, X.; Peng, Y.; Xiao, W.
199 Global warming will largely increase waste treatment CH₄ emissions in Chinese megacities:
200 insight from the first city-scale CH₄ concentration observation network in Hangzhou, China.
201 Atmos. Chem. Phys. 2023, 23, 4501–4520 DOI: 10.5194/acp-23-4501-2023,.

202 (6) Yin, Y.; Qi, X.; Gao, L.; Lu, X.; Yang, X.; Xiao, K.; Liang, P. Quantifying Methane Influx
203 from Sewer into Wastewater Treatment Processes. Environ. Sci. Technol. 2024, DOI:
204 abs/10.1021/acs.est.4c00820.

205 (7) Zhao, X.; Jin, X. K.; Guo, W.; Zhang, C.; Shan, Y. L.; Du, M. X.; Li, Y. P. China's urban
206 methane emissions from municipal wastewater treatment plant. Earth's Future. 2019, 7 (4),
207 480-490 DOI: 10.1029/2018EF001113

208 (8) Hao, X.D.; Sun, Q.; Li, J.; Yuan T.G. Factors affecting methane production in drainage
209 pipelines and their estimation methods. China's Water Supply And Drainage. 2022, 38 (20),
210 1-7 DOI: 10.19853/j.zgjsps.1000-4602.2022.20.001.

211

212

213

214

215

216

217

218

219

220

221